A direct-write, resistless hard mask for rapid nanoscale patterning of diamond

By Warren McKenzie**, John Pethica* and Graham Cross*

*Centre for Research on Adaptive Nanostructures and Nanodevices (CRANN)
School of Physics
Trinity College
Dublin 2
Ireland

** Electron Microscope Unit,
UNSW Analytical Centre
The University of New South Wales
NSW 2052 (Australia)
E-mail: WRMcKenzie@bigpond.com

We introduce a simple, resist-free dry etch mask for producing patterns in diamond, both bulk and thin deposited films. Direct gallium ion beam exposure of the native diamond surface to doses as low as 10^{15} cm^{-2} forms a top surface hard mask resistant to both oxygen plasma chemical dry etching and, unexpectedly, argon plasma physical dry etching. Gallium implant hard masks of nominal 50 nm thickness demonstrate oxygen plasma etch resistance to over 450 nm depth, or 9:1 selectivity. The process offers significant advantages over direct ion milling of diamond including increased throughput due to separation of patterning and material removal steps, allowing both nanoscale patterning resolution as well as rapid masking of areas approaching millimetre scales. Retention of diamond properties in nanostructures formed by the technique is demonstrated by fabrication of specially shaped nanoindenter tips that can perform imprint pattern transfer at over 14 GPa pressure into gold and silicon surfaces. This resistless technique can be applied to curved and non-planar surfaces for a variety of potential applications requiring high resolution structuring of diamond coatings.

1. Introduction

Diamond nanostructures have been produced that exploit some of the material's superlative properties including, for example, its high mechanical rigidity and strength for MEMS [1, 2] and nanoimprint templates [3], its high thermal conductivity for optoelectronic thermal management systems [4, 5] and power electronics [6], and its chemical inertness for electrochemical [7] and biocompatible devices [8, 9]. Patterning of these structures can be achieved by well-established resist mask-and-etch techniques or subtractive ion beam milling. In this letter we introduce a new, robust mask for efficient patterning of diamond. A low dose exposure of the native surface by an energetic gallium ion beam forms a barrier of high selectivity to subsequent plasma etching. At low aspect ratio we demonstrate dense 25 nm line features, while at intermediate (1:1) aspect ratio, 400 nm features are demonstrated with sharp corners and smooth sidewalls.

The diamond hard masking effect is related to ion top surface imaging, a recently demonstrated nanoscale patterning technique for silicon where direct exposure to an ion beam modifies an "imaging" layer at the sample surface. For silicon, the imaging layer can be formed at a specialized, ultrathin resist layer or, simply, at the native surface itself. In the former case the imaging layer is used to process an intermediate conventional thick resist etch barrier [10], while in the latter, a high performance barrier is formed for certain deep reactive ion etch conditions [11]. Our diamond hard mask is a resist-free top surface image, which functions against both reactive (oxygen) and purely physical (argon) plasma etch conditions. It offers significant advantages over direct ion milling of diamond including increased throughput and potentially better resolution and sidewall angle control due to separation of patterning and material removal steps. Limitations of resist-based processing of diamond, including planar substrate requirements and overall process complexity, are further ameliorated by the direct write, direct masking approach.

2. Experimental

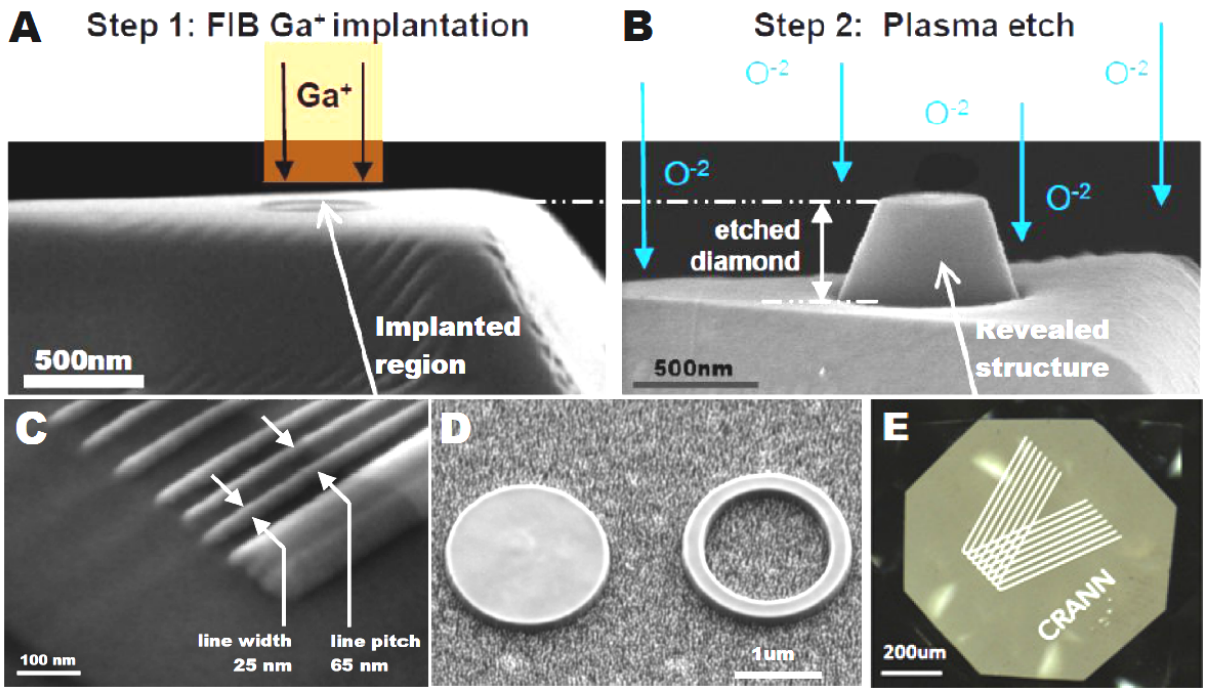

FIG. 1. Process summary and features of gallium implant diamond masking. A boron doped, single crystal synthetic diamond is implanted by gallium ions (A) forming a direct-write, negative tone mask for oxygen plasma dry etching (B) which reveals a truncated conical flat punch indenter nanostructure. Lines to 25 nm width, 65 nm pitch are fabricated (C) in singe crystal diamond. In (D), larger area features are etched into a nanocrystalline diamond on silicon (DOS) film, while in (E) a large ~ 1 mm^2 area pattern is etched in positive relief on a facet of a natural diamond gemstone. Images (A) and (B) are oriented near perpendicular, and (C) and (D) oriented at 52º to the normal of the patterned surfaces.

To illustrate the technique, panels A and B of Fig. 1(A and B) show the two steps involved in the formation of a truncated conical flat punch diamond nanostructure in boron doped (10^{21} cm^{-3}), synthetic high-temperature high-pressure (hthp) diamond crystal used for nanoindentation. First, a focused ion beam (FIB, FEI Strata 240) was used to implant a region of the native diamond surface with 30 kV Ga^+ ions below the threshold for milling, in this case to a dose of 7.5×10^{15} cm^{-2}. Then, in step 2, the sample was transferred to a dry etch tool and the surface exposed to an energetic plasma. This reveals the latent image of the FIB exposure by selective removal of diamond material below unexposed (unmasked) regions. The plateau of the structure is a flat circular surface 400 nm in diameter created by a radial FIB exposure to form the hard mask. Feature relief of 450 nm was achieved by etching the

sample for 35 minutes using a Diener "Pico" plasma etcher in pure O_2 atmosphere at 150 mTorr pressure operating at 40 kHz, 160 W power. Note the smooth etch walls, sharp corners, and lack of mask undercut in the etched structure. High resolution line features of 25 nm at 65 nm pitch are demonstrated in Fig. 1C. We have applied the technique to diamond-on-silicon thin films (Fig. 1D), as well as over large areas (1 mm) on natural gemstones as shown in Fig. 1E.

3. Results and Discussion

Unlike standard FIB processing, the production of vertical relief here is independent of the total area and complexity of patterns. We have achieved etching rates of the masked diamond of up to several 100 nm per minute, thus the throughput of this simple two-step, low ion dose process should be comparable to standard electron beam lithography processing of resists, which is limited by patterning time.

To characterize the masking process, we have analysed a cross section of a patterned structure by scanning transmission electron microscope (STEM) imaging using a high annular angle dark field (HAADF) signal, selected area electron diffraction (SAED), and energy dispersive X-ray (EDX) spectral analysis. Cross sectional STEM samples were prepared using a FIB-based in-situ lift-out technique, including a 3 kV Ga^+ beam final polishing step, using a Zeiss NVision 40 CrossBeam facility. STEM images (Fig. 2) were obtained using a custom built aberration-corrected, cold field emission VG STEM (SuperSTEM 1, SuperSTEM Laboratories, Daresbury UK) operating at 80 kV. SAED images (insets in Fig 2. A) were obtained using a JEOL 3000F field emission TEM operating at 300 kV.

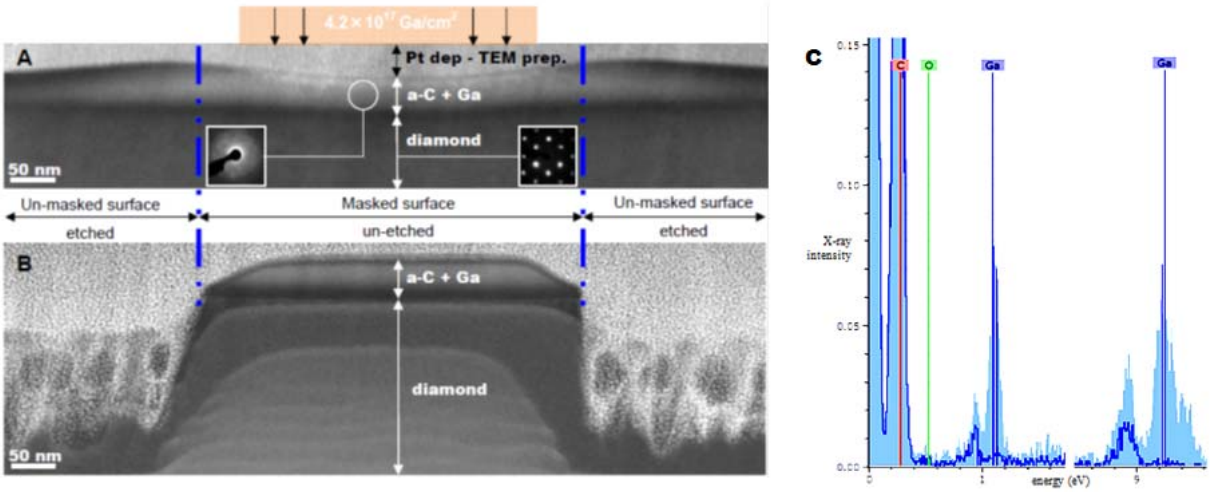

FIG. 2. High annular angle dark field scanning transmission electron microscopy images from cross sections of procesed single crystal diamond samples: (A) Immediately after Ga^+ ion implantation over the nominal surface indicated. Selected area electron diffraction (SAED) patterns of the underlying diamond and implanted surface layer are shown as insets. (B) Following oxygen plasma etch of a sample implanted identically to A. (C) Energy Dispersive X-ray spectra taken by TEM of the same areas defined for the SAED patterns in A: Implanted a-C+Ga (light blue solid spectra) regions confirm the presence of gallium, while the underlying diamond (dark blue line spectra) shows absence of Ga.

Fig. 2A shows a STEM cross sectional image of an hthp diamond surface with 30 kV, 4.2×10^{17} cm^{-2} Ga^+ FIB exposure across the region indicated in orange. Fig. 2B shows a similar sample with identical gallium ion exposure followed by oxygen plasma etching. Both samples reveal a crystalline bulk region (labeled “diamond” in Fig. 2A) characterized by an SAED pattern of its [110] zone axis (inset), and a distinct ~50 nm thick surface layer exhibiting an SAED pattern of a diffuse halo (Fig. 2A insets in overlay) indicating it is amorphous. Slightly tapered but nevertheless sharp sidewalls can be seen in Fig. 2B, together with cross sections of the slender pillars (grass) that develop in the peripheral etched regions. The grassy pillars are an artifact of the etching process arising from impurity micromasking , and can be controlled and/or eliminated by appropriate choice of etching gas mixtures12].

EDX spectra in Fig. 2C show FIB-exposed diamond rich in Ga (light blue solid spectrum), and the unexposed surface regions (dark blue line spectrum) absent in Ga. For STEM/HAADF images of Fig. 2A and 2B, this result explains the z-contrast between the layer containing only carbon (n = 6) appearing dark and regions rich in the relatively high

atom number gallium (n = 31) appearing light. Considering a vertical profile through the a-C + Ga layer for Fig. 2A and 2B we see brighter contrast from a Ga rich composition which reduces with depth towards the diamond interface. This similarity between the a-C + Ga layers in each case suggests that the composition of this phase is not noticeably affected by the plasma treatment. Considering a lateral profile across the amorphous carbon (a-C) top layer in Fig. 2A we see a continuous gallium distribution beyond the nominal beam waist (indicated in orange) which we believe is a result of overspray of the Ga^+ beam.. We note that the etch barrier remains sharply defined in Fig. 2B with feature definition significantly better than might be expected by the apparent gallium implantation profile.

We propose that the ~50 nm a-C+Ga layer containing a threshold concentration of gallium forms the plasma etch mask. The thickness of most of the mask layer appears unchanged to within the ~2 nm resolution of the images in Fig. 2. Thus, the 200 nm etch in Fig. 2B suggests a relative oxygen plasma etch rate of diamond to a-C+Ga mask of at least 100:1. There does appear to be a slight etching of the mask at its periphery; The more pronounced thinning on the left may explain the extra sidewall taper on this side of the structure.

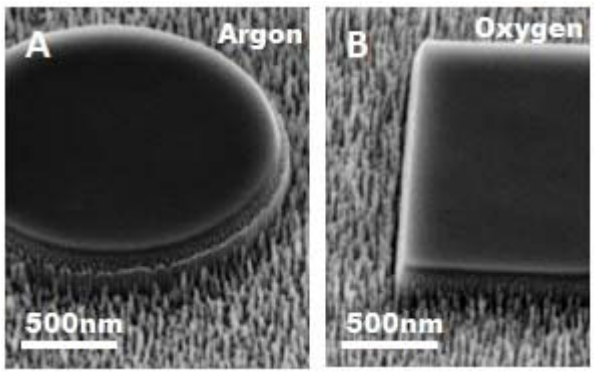

FIG. 3. Comparison of diamond ion implant mask (dose of 2.1×10^{17} cm^{-2}) performance under (A) argon plasma and (B) oxygen plasma etching of an ultrananocrystalline diamond thin film.

The gallium implanted diamond mask is effective across a wide variety of processing conditions. We have demonstrated the process using a lower FIB accelerating voltage of 10kV and expect even lower values will also be effective. These lower voltage exposures will

reduce the Ga^+ penetration into the diamond leading to a thinner "a-C + Ga" layer, which may be desirable for thinner substrates or where gallium contamination is an issue for the patterned structures functionality. We have also demonstrated the process on three types of plasma etch tools, using gas mixtures ranging from pure O_2, to O_2/CF_4 and O_2/SF_6 mixtures, to pure Ar. In all cases, we can form structures with features similar to those already presented here using an oxygen plasma etch.

In Fig. 3 argon etching is constrasted with oxygen etching. Both images share the similar feature relief from the implant mask areas and grassy roughness structures in the non-implanted (ie. etched) areas. This similarity suggests that 1) the masking mechanism is similar for etches using both plasmas, and 2) the mask is effective against physical sputtering, the only etching mechanism possible in the chemically inert Ar plasma. With a higher surface binding energy (SBE) of 7.4eV, diamond should have a significantly lower sputtering etch rate than any of the components which could be expected to be present in the mask such as Ga (SBE = 2.82eV), Ga_2O_3 (SBE for O = 2.00) or amorphous carbon (SBE = 2.00) [13]. This physical selectivity contrasts with the chemical selectivity thought to be responsible for the masking of gallium implanted silicon surfaces, where a relatively pure 5-10 nm top surface layer of Ga_2O_3 has been shown by TOF-SIMS to form during reactive ion etching in oxygen plasma [14]. We suspect that a conversion of sp3 to sp2 bond hyrbridization to be playing a role in the etch contrast, and are carrying out further investigation of this hypothesis.

Diamond is traditionally used in nanoindentation testing because of its extremely high mechanical strength and stiffness, and low surface energy (giving low adhesion, friction and chemical reactivity). We have used our masking technique to produce novel diamond nanoindentation dies for direct imprint patterning of hard materials at room temperature. For broader nanoimprint manufacturing applications [15], diamond provides superior overall

mechanical robustness to industry standard quartz or silicon dies, and may yield lower fouling rates due to adhesive transfer. These are critical factors reducing die imprint cycle lifetimes which currently impede the adaption of nanoimprint as an economically viable fabrication technique.

In Fig. 4A a complex pattern formed by gallium implant mask at the apex of a single crystal diamond nanoindenter tip is shown. A modified nanoindenter setup (MTS Nano Instruments XP) was used to imprint this pattern and monitor the mechanical behavior (load and displacement) in real time [16]. The sharply defined diamond die features of Fig. 4A are replicated with a deep (~300 nm) imprint into a gold thin film in Fig. 4B. Fig. 4C shows a shallow imprint into a much harder silicon surface, again at room temperature. In both instances, all features of the die are well reproduced including the ~100 nm pitch line structures. Fig. 4D demonstrates cyclic loading of the die with an array of 6 imprints into a silicon each taken to a maximum contact pressure of 14.6 GPa. The die features are replicated without any signs of damage or wear. The implanted diamond retains its exceptional mechanical properties.

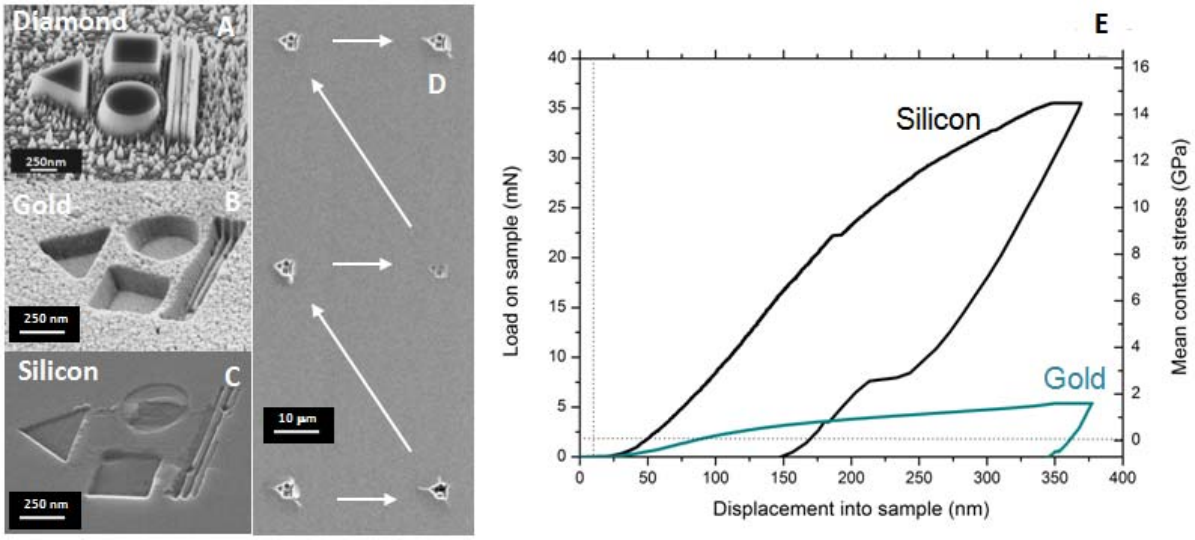

FIG. 4. Room temperature indentation of a diamond nanoimprint die as-patterned by the gallium implant mask (A) into solid materials including gold (B) and silicon (C). In (D) an array of six consecutive imprints into silicon was made with peak mean imprint stress of 14.6 GPa. Indentation load vs. displacement mechanics were measured by a nanoindenter (E).

3. Conclusions

We have presented a simple direct-write means of fabricating nanoscale structures on diamond surfaces. The new process is based on surface modifications induced by a Ga^+ focused ion beam which forms a high resolution dry etch mask. TEM analysis of ion implanted diamond and etch structures have identified the mask as an amorphous carbon layer ~50 nm in thickness and rich in gallium. The mask was found to be effective against both reactive and non-reactive ion species indicating a strong physical component to the masking effect. While investigation and optimization to determine the ultimate resolution, side wall angle control, and aspect ratio remain to be performed, scaling of feature size was shown with patterns ranging from 25 nm to sub-millimeter width. The highest resolution line structures appear to be limited by the FIB probe size. A specialized nanoimprint application was demonstrated with the reproduction of features less than 100 nm by imprinting a patterned diamond die into both silicon and gold.

Acknowledgement

This material is based upon work supported by Science Foundation Ireland Grants 08/IN.1/I1932, 00/PI.1/C028 and CRANN CSET Grant. The authors also acknowledge financial support from the European Union Framework 6 program, Integrated Infrastructure Initiative, Reference 026019 ESTEEM. We thank Roseanne Reilly of CRANN for assistance in performing nanoindentation. and acknowledge the valuable assistance at the SuperSTEM laboratories at Daresbury UK with Dr. Mhairi Gass, and at the University of Oxford (UK) with Dr. Lisa Karlsson and Dr. Gareth Hughes.

References

[1] A.V. Sumant, O. Auciello, R.W. Carpick, S. Srinivasan, J.E. Butler, Ultrananocrystalline and Nanocrystalline Diamond Thin Films for MEMS/NEMS Applications. Mrs Bulletin, 35 (2010) 281-288.

[2] N. Moldovan, R. Divan, H.J. Zeng, J.A. Carlisle, Nanofabrication of sharp diamond tips by e-beam lithography and inductively coupled plasma reactive ion etching. Journal of Vacuum Science & Technology B, 27 (2009) 3125-3131.

[3] J. Taniguchi, Y. Tokano, I. Miyamoto, M. Komuro, H. Hiroshima, Diamond nanoimprint lithography. Nanotechnology, 13 (2002) 592-596.

[4] A. Harkonen, S. Suomalainen, E. Saarinen, L. Orsila, R. Koskinen, O. Okhotnikov, S. Calvez, M. Dawson, 4 W single-transverse mode VECSEL utilising intra-cavity diamond heat spreader. Electron. Lett., 42 (2006) 693-694.

[5] A.J. Maclean, R.B. Birch, P.W. Roth, A.J. Kemp, D. Burns, Limits on efficiency and power scaling in semiconductor disk lasers with diamond heatspreaders. Journal of the Optical Society of America B-Optical Physics, 26 (2009) 2228-2236.

[6] Y. Gurbuz, O. Esame, I. Tekin, W.P. Kang, J.L. Davidson, Diamond semiconductor technology for RF device applications. Solid-State Electronics, 49 (2005) 1055-1070.

[7] A. Qureshi, W.P. Kang, J.L. Davidson, Y. Gurbuz, Review on carbon-derived, solid-state, micro and nano sensors for electrochemical sensing applications. Diamond and Related Materials, 18 (2009) 1401-1420.

[8] C.E. Nebel, B. Rezek, D. Shin, H. Uetsuka, N. Yang, Diamond for bio-sensor applications. Journal of Physics D-Applied Physics, 40 (2007) 6443-6466.

[9] R.J. Hamers, Nanotechnology - Diamonds are for tethers. Nature, 454 (2008) 708-709.

[10] K. Arshak, M. Mihov, D. Sutton, A. Arshak, S.B. Newcomb, Negative resist image by dry etching: a novel surface imaging resist scheme. Microelectronic Engineering, 67-8 (2003) 130-139.

[11] N. Chekurov, K. Grigoras, A. Peltonen, S. Franssila, I. Tittonen, The fabrication of silicon nanostructures by local gallium implantation and cryogenic deep reactive ion etching. Nanotechnology, 20 (2009).

[12] Y. Ando, Y. Nishibayashi, K. Kobashi, T. Hirao, K. Oura, Smooth and high-rate reactive ion etching of diamond. Diamond and Related Materials, 11 (2002) 824-827.

[13] J. F. Ziegler, M. D. Zeigler, J. P. Biersack, in: SRIM-2008.03, 2008.

[14] B. Schmidt, S. Oswald, L. Bischoff, Etch rate retardation of Ga+-ion beam-irradiated silicon. Journal of the Electrochemical Society, 152 (2005) G875-G879.

[15] G.L.W. Cross, The production of nanostructures by mechanical forming. Journal of Physics D-Applied Physics, 39 (2006) R363-R386.

[16] G.L.W. Cross, B.S.O. Connell, J.B. Pethica, H. Rowland, W.P. King, Variable temperature thin film indentation with a flat punch. Review of Scientific Instruments, 79 (2008).